

Revealing the Microscopic Mechanism of Displacive Excitation of Coherent Phonons in a Bulk Rashba Semiconductor

P. Fischer¹, J. Bär¹, M. Cimander¹, L. Feuerer¹, V. Wiechert¹, O. Tereshchenko², and D. Bossini¹

¹*Department of Physics and Center for Applied Photonics,
University of Konstanz, D-78457 Konstanz, Germany*

²*Rzhanov Institute of Semiconductor Physics,
Siberian Branch, Russian Academy of Sciences*

(Dated: October 11, 2024)

Changing the macroscopic properties of quantum materials by optically activating collective lattice excitations has recently become a major trend in solid state physics. One of the most commonly employed light-matter interaction routes is the displacive mechanism. However, the fundamental contribution to this process remains elusive, as the effects of free-carrier density modification and raised effective electronic temperature have not been disentangled yet. Here we use time-resolved pump-probe spectroscopy to address this issue in the Rashba semiconductor BiTeI. Exploring the conventional regime of electronic interband transitions for different excitation wavelengths as well as the barely accessed regime of electronic intraband transitions, we answer a long-standing open question regarding the displacive mechanism: the lattice modes are predominantly driven by the rise of the effective electronic temperature. In the intraband regime, which allows to increase the effective carrier temperature while leaving their density unaffected, the phonon coherence time does not display significant fluence-dependent variations. Our results thus reveal a pathway to displacive excitation of coherent phonons, free from additional scattering and dissipation mechanisms typically associated with an increase of the free-carrier density.

I. INTRODUCTION

The generation of coherent phonons through laser pulses has recently been established as a means to both control [1–4] and probe [5, 6] the macroscopic phases of quantum materials. Impulsive processes are one of the most popular approaches to the optical excitation of coherent lattice dynamics. In particular, they allow to excite longitudinal optical (LO) phonons which are symmetrically inaccessible to resonant dipolar excitation. In general, a distinction is drawn between two methods: If light couples to the electronic system non-resonantly, coherent phonons are induced by impulsive stimulated Raman scattering. On the other hand, if the optical stimulus is resonant with the electronic system, displacive excitation of coherent phonons (DECP) is realized [7, 8]. The established theory of DECP [9] describes the generation of coherent lattice modes in terms of two contributions, namely the increase of the charge-carrier density n_c and the rise in the effective temperature of the electronic subsystem T_e . Crucially, so far neither theory nor experiment could disentangle these two contributions. From an experimental point of view, typical DECP experiments involve pump photon energies resonant with electronic interband transitions. Therefore, in the absorption process both n_c and T_e are increased. However, modern pulsed lasers can operate in the mid-infrared regime, with photon energies lower than the band gap of most solids. These light sources can therefore be employed to pump electronic intraband transitions selectively, which raises only T_e and keeps n_c constant. Hence, mid-infrared lasers offer the possibility to address the fundamental question about the micro-

scopic mechanism of DECP, which has been unresolved for more than 30 years [9].

We study the excitation of coherent phonons in BiTeI, a prototypical Rashba semiconductor, via pump-probe time-domain reflection spectroscopy. The band structure of this material is ideal for a quantitative comparison of interband and intraband DECP. Due to the narrow band gap, BiTeI absorbs light well into the near-infrared spectral range via electronic interband transitions. The high intrinsic carrier density combined with the huge Rashba spin splitting ($\Delta\varepsilon \approx 100$ meV) of the lowest conduction band allows intraband transitions in the mid-infrared regime [10].

Our experiments reveal that in the interband regime the phonon coherence time is not affected up to an optically doped carrier density of $n_c \approx 1 \cdot 10^{21}$ cm⁻³. These findings demonstrate that BiTeI is a surprisingly robust material for coherent phononics. This result is remarkable, considering that in other semiconductors (GaAs, GaP, InAs, InSb) the coherence time is typically suppressed by carrier densities orders of magnitude smaller than in BiTeI [11–14]. Strikingly in the intraband regime the amplitude of the phonons linearly increases with the laser fluence, even though n_c remains constant. Even more tantalizing, the phonon coherence time remains unaffected, even if the laser fluence is set to a value one order of magnitude higher than in the case electronic interband pumping.

II. MATERIALS AND METHODS

Our BiTeI specimen was grown by a modified Bridgman method using a rotating heat field [10]. Its layered structure is built from covalently bound bilayers formed by $(\text{BiTe})^+$ which ionically bond to $(\text{I})^-$ and thus form trilayers. These trilayers in turn are stacked by van der Waals forces. We are investigating interband and intraband DECP in BiTeI via pump-probe time-domain reflection spectroscopy. Therefore, we are interested in phonons with A_1 symmetry [9]. As demonstrated by spontaneous Raman scattering [15], BiTeI features an A_1 mode at a center frequency of 2.7 THz. Its corresponding atomic displacement is shown in Fig. 1 (a). To perform our experiments, we employ two different amplified laser systems emitting fs pulses at kHz repetition rates (details in [16]). A commercial system delivers laser pulses with photon energies tunable in the visible and near-infrared ranges (0.5 eV - 3 eV, 2 μm - 400 nm). A self-built system [17] generates pulses in the mid-infrared (0.18 eV, 7.0 μm). Thus, we are able to employ photon energies both above and below the fundamental band gap of BiTeI (band-gap energy $\varepsilon_g \approx 0.38$ eV [18]). In all our experiments, the central wavelength of the probe beam is 1.2 μm (photon energy ≈ 1 eV). The reflected probe beam is recollimated and detected by two photodiodes in a balanced detection scheme. The signal is acquired via a digital lock-in method. The sample was always at room temperature.

Figure 1 (b) depicts the electronic band structure of BiTeI. The compound is classified as a degenerate n-type semiconductor, implying that its Fermi energy ε_F lies above the conduction-band minimum [18] (black dashed line). Because of the Rashba effect [19], the dispersion of electrons with antiparallel spins is displaced in opposite directions from the center of the Brillouin zone. The resulting energy splitting measured from the bottom of the conduction bands to their intersection is $\Delta\varepsilon \approx 100$ meV (green dashed lines) [18]. Consequently, the absorption properties are characterized by two electronic transitions. With β we represent the highest-energy intraband transition between the Rashba-split conduction bands [20] (red arrow). The lowest-energy interband transition, promoting electrons from the highest valence band to an unoccupied state above ε_F in the lowest conduction band, is denoted by γ (blue arrow). To determine the energies of these two transitions we measure the transmission spectrum of our sample (details in [16]) and obtain $\beta = 0.37$ eV (3.35 μm) and $\gamma = 0.52$ eV (2.39 μm). Depending on the crystal-growth conditions, the intrinsic charge-carrier density n_i of BiTeI can vary considerably. Since γ depends on ε_F , it is sensitive to n_i . Comparing the experimentally obtained value of γ to the literature [22], we estimate the intrinsic carrier density in our sample to be $n_i = 6 \cdot 10^{19} \text{ cm}^{-3}$.

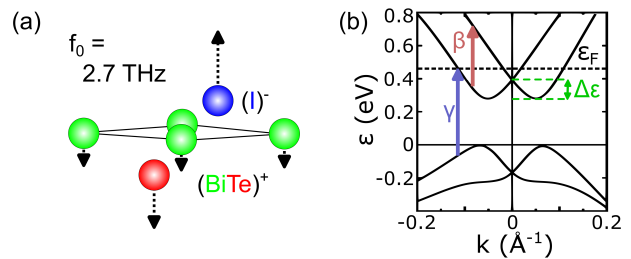


FIG. 1. (a) Atomic displacement and central frequency of an A_1 phonon mode in BiTeI [15]. (b) Rashba-split band structure of BiTeI (adapted from [21], $\Delta\varepsilon = 100$ meV). The transition β (red dashed line at 0.37 eV) represents the highest-energy intraband transition. The transition γ (blue dashed line at 0.52 eV) is the lowest-energy interband transition corresponding to the electronic excitation from the valence band to a free state above the Fermi energy ε_F (dashed black line).

III. RESULTS AND DISCUSSION

The main scientific goal of our work is to unravel the microscopic nature of DECP. We begin by characterizing the canonical regime of the displacive mechanism, in which the excitation of electronic interband transitions increases both n_c and T_e .

Figure 2 (a) shows the dynamics of the normalized transient reflectivity $\Delta R/R_0$ induced by laser pulses with a central wavelength of 520 nm. The pulse duration is 200 fs and the fluence is set to $\Phi = 1.39 \text{ mJ/cm}^2$. The signal consists of two components, (i) harmonic oscillations with a period on the femtosecond timescale superimposed to (ii) an exponential decay on the picosecond timescale with an amplitude of $\Delta R/R_0 \approx 1.5 \cdot 10^{-2}$. Calculating the power spectrum via Fourier transform (Fig. 2 (b)) reveals that the central frequency of the oscillations is 2.76 THz, a value consistent with the A_1 mode, whose atomic displacement corresponds to the out-of-phase oscillations of $(\text{BiTe})^+$ and $(\text{I})^-$ [15] (Fig 1 (a)). We ascribe the exponential contribution to the signal to the thermalization of the photo-excited electrons with acoustic phonons [23].

Analyzing the isolated oscillatory component of $\Delta R/R_0$ (details in [16], green circles in Fig. 2 (c)) we obtain that the amplitude of the oscillations amounts to approximately $0.72 \cdot 10^{-3}$. To determine the coherence time τ_c , we calculate the power spectrum shown by the green circles in Fig. 2 (d) via Fourier transform and fit it with a Lorentzian function (details in [16]). We find $\tau_c = (5.7 \pm 0.1) \text{ ps}$. This result is in good agreement with the value obtained by spontaneous Raman scattering (6 ps) [15]. In contrast to the experiment reported in [15], however, we set the fluence Φ to a

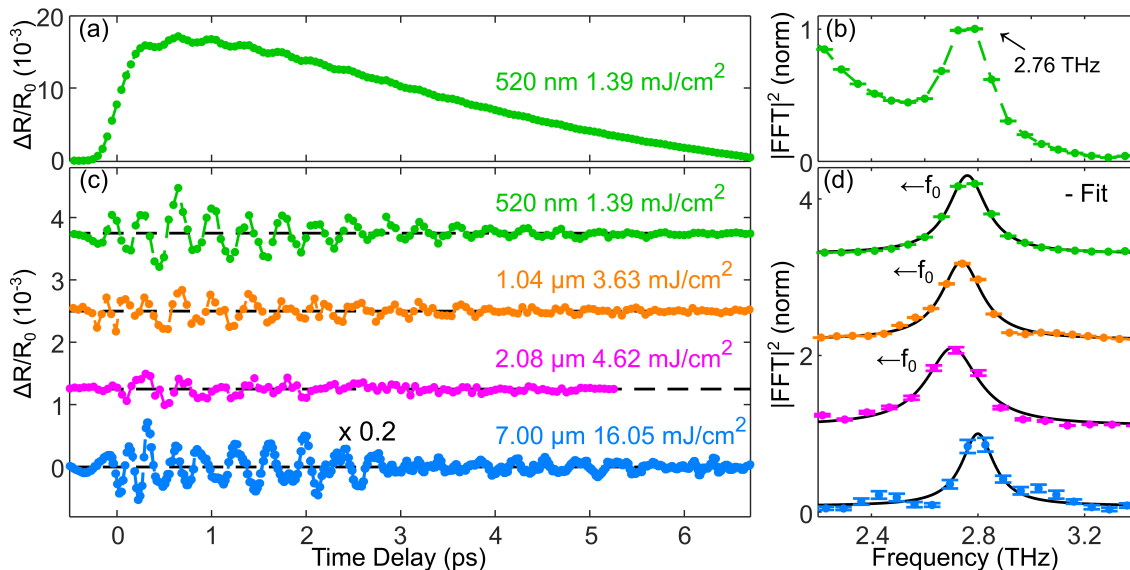


FIG. 2. (a) Dynamics of the normalized reflectivity of BiTeI induced by 520-nm laser pulses. The fluence was set to 1.39 mJ/cm^2 . (b) Power spectrum of the time trace shown in panel (a), obtained via Fourier transform. (c) Oscillatory component of the transient reflectivity for pump wavelengths spanning the visible, near-infrared and the mid-infrared spectral ranges after subtraction of the incoherent background. Note that for the 7.00- μm data (blue), the time trace was scaled with a factor of 0.2 for presentation purposes. (d) Power spectra of the time traces shown in panel (c). Each data set is normalized on its peak value at the respective central frequency f_0 . The solid black lines represent a fit with a Lorentzian function (details in [16]). For interband excitation (520 nm - 2.08 μm) f_0 redshifts with increasing fluence (see explanation in the main text).

value that significantly increases the free-carrier density n_c . Our analysis shows that this has no effect on τ_c , which is at first surprising since LO phonons usually interact strongly with free electrons [24]. Driven by this finding, from Φ we calculate the excitation density, i.e. an estimate of the density of photons absorbed by electrons assuming that a single electron absorbs a single photon (details in [16]). We highlight that in the interband regime the excitation density is equal to the increase of n_c , i.e. the semiconductor is optically doped. This procedure results in $n_c \approx 4 \cdot 10^{20} \text{ cm}^{-3}$, a value almost one order of magnitude larger than the intrinsic charge-carrier density n_i . In comparison to III-V semiconductors (GaAs, GaP, InAs, InSb) [11–14], this behaviour is remarkable. For example, in GaAs free carriers with a density three orders of magnitude smaller strongly suppress the coherence time of the lattice oscillations [14]. We attribute this difference to the van der Waals structure of BiTeI, due to which the electron wave vector is confined to the plane perpendicular to the stacking axis for states close to the conduction-band minimum. The wave vector of LO phonons with A_1 symmetry, however, is parallel to the stacking. Thus, the emission and absorption of such phonons by free electrons is suppressed due to the restrictions of energy and momentum conservation.

Motivated by this observation, we quantitatively analyze the phononic robustness with respect to the excitation density. For this purpose, we experimentally

vary the pump fluence Φ . For each value of Φ we estimate the excitation density and analyze the amplitude A_0 and the coherence time τ_c of the oscillations from the Lorentz fit (details in [16]). The results are shown in Fig. 3 (a) and (b) by the green circles. The amplitude A_0 of the phononic contribution to the signal (Fig. 3 (a)) scales linearly with the excitation density, which is consistent with DECP [25]. The value of τ_c (Fig. 3 (b)), on the other hand, shows no significant density-dependent variations up to $n_c \approx 4 \cdot 10^{20} \text{ cm}^{-3}$.

Despite the scientific interest, we cannot further increase the fluence of the 520-nm pump beam, since the sample damage threshold would be surpassed. We thus tune the central wavelength to 1.04 μm . The difference between excitation at 520 nm and 1.04 μm is that the excited electrons have less excess energy in the latter case (i.e. the energy difference between the excited state and the bottom of the conduction band). On the one hand, this allows us to further increase the fluence, as the damage threshold is higher compared to the 520-nm excitation. Therefore, we can analyze τ_c at even higher carrier densities. However, this also means that the electronic subsystem reaches a lower value of T_e after internal thermalization. This in turn allows us to investigate how the phononic amplitude A_0 is affected when T_e is lower but n_c is comparable to the 520-nm excitation. We will first address the latter aspect. To begin with, with excitation at 1.04 μm we can increase the laser fluence to up to 3.63 mJ/cm^2 , which

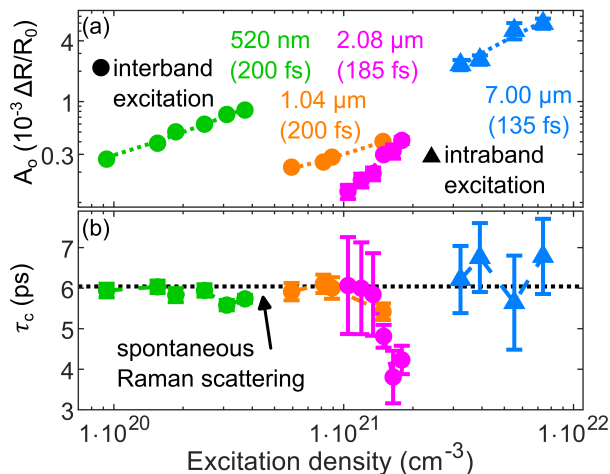


FIG. 3. Dependence of the phononic oscillation parameter on the excitation density. Pump wavelengths (pulse durations) are indicated in the top panel. The error bars represent the 95% confidence interval. (a) For each measurement series, the oscillation amplitude A_o shows a linear dependence on the excitation density. The data are plotted in a double-logarithmic scale for the sake of presentation, the dotted lines represent linear fits. (b) Dependence of the coherence time τ_c on the excitation density. The value obtained via Raman spectroscopy is shown by the dashed line [15].

corresponds to an excitation density of $1.5 \cdot 10^{21} \text{ cm}^{-3}$. The oscillatory time trace of $\Delta R/R_0$ and the corresponding power spectrum measured at this highest fluence are shown in Fig. 2 (c) and (d). The results of the excitation-density dependence analysis (orange circles in Fig. 3 (a) and (b)) show that the amplitude A_o scales linearly with the excitation density as in the case of the 520-nm pump beam, however with smaller values. In fact, considering comparable values of the excitation density ($4 - 6 \cdot 10^{20} \text{ cm}^{-3}$), A_o is 3.6 times bigger in the data set obtained with the 520-nm pump beam. Thus, we infer that the rise in T_e is indeed a major factor for DECP. With regards to τ_c we observe a reduction of the parameter value by about 10% at the highest excitation density ($1.5 \cdot 10^{21} \text{ cm}^{-3}$).

To further investigate the matter we set the pump-pulse central wavelength to 2.08 μm (purple in Fig. 2 (c)-(d) and Fig. 3 (a) and (b)). In comparison to the 1.04- μm excitation, the values of A_o in the 2.08- μm data are lower, as expected, but the slope is bigger. This can be attributed to the different durations of the pump pulses, 200 fs at 1.04 μm compared to 185 fs at 2.08 μm . The closer the temporal profile of the excitation pulses is to a delta function, the more efficient DECP is [25].

As far as τ_c is concerned, a decrease down to 38% of the equilibrium value is observed at an excitation density of approximately $1.8 \cdot 10^{21} \text{ cm}^{-3}$ (see Fig. 3 (b)), a value corresponding to $\Phi = 4.62 \text{ mJ/cm}^2$. This

decrease can also be seen in the time trace shown in Fig. 2 (c) and in the broader power spectrum depicted in Fig. 2 (d). Conversely, we have demonstrated that BiTeI can maintain the coherence time of the A_1 phonon mode up to an optically doped carrier density of $n_c \approx 1 \cdot 10^{21} \text{ cm}^{-3}$.

The eigenfrequency of A_1 mode redshifts as the excitation density increases (see Fig. 2 (d)). It decreases by approximately 2% when comparing the values at the highest excitation densities between the 520-nm and 2.08- μm data. This renormalisation of the lattice eigenfrequency stems from the screening of the ionic charges by the additional free charge carriers [26].

So far, we have demonstrated that BiTeI is phononically robust and that the rise in T_e plays a major role in DECP. However, pumping electronic interband transitions we could not completely disentangle the contribution of the rise in T_e from the increase of n_c to the phonon excitation. Therefore, we employ pump pulses in the mid-infrared range with a central wavelength of 7.00 μm . The corresponding photon energy (0.18 eV) is not high enough to induce interband excitation and thus cannot change n_c . However, mid-infrared pump pulses excite intraband transitions between the Rashba-split conduction bands (red arrow in Fig. 1 (b)). Consequently, we can further increase Φ in comparison to previous measurements without damaging the sample. In fact, we can employ fluences up to 16.1 mJ/cm^2 , nearly four times higher than for 2.08- μm excitation and even one order of magnitude higher than for 520-nm excitation. This translates to excitation densities up to approximately $7.4 \cdot 10^{21} \text{ cm}^{-3}$. We emphasize that the interpretation of the excitation density in the intraband regime is restricted to density of absorbed photons and explicitly does not include the simultaneous increase of n_c as in the interband regime. Nevertheless, the time-domain data (Fig. 2 (c)) and the corresponding power spectrum (Fig. 2 (d)) disclose that coherent phonons are excited even when n_c remains constant. Combined with the conclusions of electronic interband pumping, this compelling observation closes the fundamental issue standing for 30 years regarding the microscopy of DECP: the rise in T_e and not the increase of n_c is the dominant contribution to DECP.

The amplitude retains its linear dependence on the fluence (blue triangulars in Fig. 3 (a)). From the absence of non-linearity in A_o , we conclude that a single photon excites a single electron for intraband excitation as well. A saturation of the amplitude due to bleaching of the electronic intraband transition could be expected, as the highest value for the excitation density is two orders of magnitude larger than n_i . However, photo-excited carriers in BiTeI scatter on a timescale shorter than 80 fs [23, 27]. As the duration of the 7.00- μm pump pulses is 135 fs, the conduction-band electrons are redistributed in momentum space within

the duration of the optical excitation, thus preventing the absorption from saturating.

In contrast to the interband regime, we observe that τ_c shows no significant excitation-density-dependent variations (blue triangular in Fig. 3 (b)). This can be attributed to the absence of additional scattering channels and energy dissipation mechanisms that typically arise with higher carrier densities. Therefore, pumping electronic intraband transitions selectively in BiTeI allows to linearly increase A_o with the fluence while avoiding shortening τ_c . Finally, we observe that in contrast to the interband regime the frequency of the A_1 phonon is not affected (see Fig. 2 (d)). As the mid-infrared pulses cannot increase n_c , no screening of the ionic charges takes place.

IV. CONCLUSION

We have demonstrated displacive excitation of coherent phonons in BiTeI. By tuning the pump central wavelength in a broad spectral range spanning the visible, near-infrared and even mid-infrared regimes we observe DECP both for electronic interband and intraband transitions. In the former scenario, we find that the phonon coherence time can be maintained for charge-carrier densities up to $n_c = 1 \cdot 10^{21} \text{ cm}^{-3}$. This demonstrates a remarkable phononic robustness, since in III-V semiconductors the coherence time is already suppressed at values of n_c orders of magnitude

lower. The scenario of intraband transitions has been so far barely explored in terms of DECP. Our data demonstrates that the photo-induced rise of T_e is the main microscopic contribution to DECP. Furthermore, in this regime we can raise the phononic amplitude by increasing the fluence, while the coherence time is unaffected. We observe that these results may be relevant for the development of optically driven ultrafast technology in quantum materials. Schemes addressing the coherent structural manipulation of solids can be based on exciting electronic intraband transitions selectively, thus avoiding the additional scattering channels and energy dissipation induced by an increase of the carrier density. Other routes, like Raman sum-frequency generation [28] and nonlinear phononics [29] are expected to induce the same phonon modes even in a nonlinear dynamical regime. This is relevant with regard to the symmetry of the 2.7 THz mode, which may allow direct modification of the Rashba coupling [30–35].

ACKNOWLEDGEMENTS

The exchange of samples took place in May 2021. The authors thank C. Beschle, and S. Eggert for their technical support. This work was supported by Deutsche Forschungsgemeinschaft (BO 5074/2-1), Davide Bossini acknowledges the support of the DFG program BO 5074/1-1.

-
- [1] K. W. Kim, A. Pashkin, H. Schäfer, M. Beyer, M. Porer, T. Wolf, C. Bernhard, J. Demsar, R. Huber, and A. Leitnerstorfer, Ultrafast transient generation of spin-density-wave order in the normal state of BaFe₂As₂ driven by coherent lattice vibrations, *Nature Materials* **11**, 497–501 (2012).
- [2] T. F. Nova, A. Cartella, A. Cantaluppi, M. Först, D. Bossini, R. V. Mikhaylovskiy, A. V. Kimel, R. Merlin, and A. Cavalleri, An effective magnetic field from optically driven phonons, *Nature Physics* **13**, 132–136 (2016).
- [3] T. F. Nova, A. S. Disa, M. Fechner, and A. Cavalleri, Metastable ferroelectricity in optically strained SrTiO₃, *Science* **364**, 1075–1079 (2019).
- [4] D. Fausti, R. I. Tobey, N. Dean, S. Kaiser, A. Dienst, M. C. Hoffmann, S. Pyon, T. Takayama, H. Takagi, and A. Cavalleri, Light-induced superconductivity in a stripe-ordered cuprate, *Science* **331**, 189–191 (2011).
- [5] S. Wall, D. Wegkamp, L. Foglia, K. Appavoo, J. Nag, R. Haglund, J. Stähler, and M. Wolf, Ultrafast changes in lattice symmetry probed by coherent phonons, *Nature Communications* **3**, 10.1038/ncomms1719 (2012).
- [6] F. Mertens, D. Mönkebücher, U. Parlak, C. Boix-Constant, S. Mañas-Valero, M. Matzer, R. Adhikari, A. Bonanni, E. Coronado, A. M. Kalashnikova, D. Bossini, and M. Cinchetti, Ultrafast coherent THz lattice dynamics coupled to spins in the Van der Waals antiferromagnet FePS₃, *Advanced Materials* **35**, 10.1002/adma.202208355 (2022).
- [7] T. K. Cheng, S. D. Brorson, A. S. Kazeroonian, J. S. Moodera, G. Dresselhaus, M. S. Dresselhaus, and E. P. Ippen, Impulsive excitation of coherent phonons observed in reflection in bismuth and antimony, *Applied Physics Letters* **57**, 1004–1006 (1990).
- [8] G. C. Cho, W. Kütt, and H. Kurz, Subpicosecond time-resolved coherent-phonon oscillations in GaAs, *Physical Review Letters* **65**, 764–766 (1990).
- [9] H. J. Zeiger, J. Vidal, T. K. Cheng, E. P. Ippen, G. Dresselhaus, and M. S. Dresselhaus, Theory for displacive excitation of coherent phonons, *Phys. Rev. B* **45**, 768 (1992).
- [10] A. A. Makhnev, L. V. Nomerovannaya, T. V. Kuznetsova, O. E. Tereshchenko, and K. A. Kokh, Optical properties of BiTeI semiconductor with a strong rashba spin-orbit interaction, *Optics and Spectroscopy* **117**, 764 (2014).
- [11] W. Kutt, G. C. Cho, T. Pfeifer, and H. Kurz, Subpicosecond generation and decay of coherent phonons in III-V compounds, *Semiconductor Science and Technology* **7**, B77–B79 (1992).

- [12] O. V. Misochko, Coherent phonons and their properties, *Journal of Experimental and Theoretical Physics* **92**, 246–259 (2001).
- [13] K. Yee, K. Lee, E. Oh, D. Kim, and Y. Lim, Coherent optical phonon oscillations in bulk GaN excited by far below the band gap photons, *Physical review letters* **88**, 105501 (2002).
- [14] M. Hase, S.-i. Nakashima, K. Mizoguchi, H. Harima, and K. Sakai, Ultrafast decay of coherent plasmon-phonon coupled modes in highly doped GaAs, *Physical Review B* **60**, 16526 (1999).
- [15] I. Y. Sklyadneva, R. Heid, K.-P. Bohnen, V. Chis, V. A. Volodin, K. A. Kokh, O. E. Tereshchenko, P. M. Echenique, and E. V. Chulkov, Lattice dynamics of bismuth tellurohalides, *Phys. Rev. B* **86**, 094302 (2012).
- [16] See Supplemental Material [URL_will_be_inserted_by_publisher] for details concerning the laser system, the analysis of the electronic background and the coherent oscillations and the optical parameters of BiTeI.
- [17] C. Schoenfeld, L. Feuerer, A. Heinrich, A. Leitenstorfer, and D. Bossini, Nonlinear generation, compression and spatio-temporal analysis of sub-GV/cm-class femtosecond mid-infrared transients, *Laser And Photonics Reviews* 10.1002/lpor.202301152 (2024).
- [18] K. Ishizaka, M. S. Bahramy, H. Murakawa, M. Sakano, T. Shimojima, T. Sonobe, K. Koizumi, S. Shin, H. Miyahara, A. Kimura, K. Miyamoto, T. Okuda, H. Namatame, M. Taniguchi, R. Arita, N. Nagaosa, K. Kobayashi, Y. Murakami, R. Kumai, Y. Kaneko, Y. Onose, and Y. Tokura, Giant rashba-type spin splitting in bulk BiTeI, *Nature Materials* **10**, 521 (2011).
- [19] E. Rashba, Semiconductors with a loop of extrema, *Journal of Electron Spectroscopy and Related Phenomena* **201**, 4–5 (2015).
- [20] L. Demkó, G. A. H. Schober, V. Kocsis, M. S. Bahramy, H. Murakawa, J. S. Lee, I. Kézsmárki, R. Arita, N. Nagaosa, and Y. Tokura, Enhanced infrared magnetooptical response of the nonmagnetic semiconductor BiTeI driven by bulk rashba splitting, *Phys. Rev. Lett.* **109**, 167401 (2012).
- [21] M. S. Bahramy, R. Arita, and N. Nagaosa, Origin of giant bulk rashba splitting: Application to BiTeI, *Phys. Rev. B* **84**, 041202 (2011).
- [22] J. S. Lee, G. A. H. Schober, M. S. Bahramy, H. Murakawa, Y. Onose, R. Arita, N. Nagaosa, and Y. Tokura, Optical response of relativistic electrons in the polar BiTeI semiconductor, *Phys. Rev. Lett.* **107**, 117401 (2011).
- [23] A. S. Ketterl, B. Andres, M. Polverigiani, V. Voroshnin, C. Gahl, K. A. Kokh, O. E. Tereshchenko, E. V. Chulkov, A. Shikin, and M. Weinelt, Effect of rashba splitting on ultrafast carrier dynamics in BiTeI, *Phys. Rev. B* **103**, 085406 (2021).
- [24] H. Fröhlich, Electrons in lattice fields, *Advances in Physics* **3**, 325 (1954).
- [25] R. Merlin, Generating coherent THz phonons with light pulses, *Solid State Communications* **102**, 207 (1997), highlights in *Condensed Matter Physics and Materials Science*.
- [26] P. Yu and M. Cardona, *Fundamentals of Semiconductors*, 3rd ed. (Springer, Berlin Heidelberg New York, 2005).
- [27] J. Mauchain, Y. Ohtsubo, M. Hajlaoui, E. Papalazarou, M. Marsi, A. Taleb-Ibrahimi, J. Faure, K. A. Kokh, O. E. Tereshchenko, S. V. Ereemeev, E. V. Chulkov, and L. Perfetti, Circular dichroism and superdiffusive transport at the surface of BiTeI, *Phys. Rev. Lett.* **111**, 126603 (2013).
- [28] D. M. Juraschek and S. F. Maehrlein, Sum-frequency ionic Raman scattering, *Physical Review B* **97**, 174302 (2018).
- [29] M. Foerst, Y. Tokura, C. Manzoni, S. Kaiser, Y. Tomioka, R. Merlin, R. Merlin, and A. Cavalleri, Non-linear phononics as an ultrafast route to lattice control, *Nature Physics* **7**, 854 (2011).
- [30] A. Crepaldi, L. Moreschini, G. Autès, C. Tournier-Colletta, S. Moser, N. Virk, H. Berger, P. Bugnon, Y. J. Chang, K. Kern, A. Bostwick, E. Rotenberg, O. V. Yazyev, and M. Grioni, Giant ambipolar rashba effect in the semiconductor BiTeI, *Phys. Rev. Lett.* **109**, 096803 (2012).
- [31] L. Cheng, L. Wei, H. Liang, Y. Yan, G. Cheng, M. Lv, T. Lin, T. Kang, G. Yu, J. Chu, Z. Zhang, and C. Zeng, Optical manipulation of rashba spin-orbit coupling at SrTiO₃-based oxide interfaces, *Nano Letters* **17**, 6534–6539 (2017).
- [32] G. Kremer, J. Maklar, L. Nicolai, C. W. Nicholson, C. Yue, C. Silva, P. Werner, J. H. Dil, J. Krem-paský, G. Springholz, R. Ernstorfer, J. Minár, L. Rettig, and C. Monney, Field-induced ultrafast modulation of rashba coupling at room temperature in ferroelectric alpha-GeTe(111), *Nature Communications* **13**, 10.1038/s41467-022-33978-3 (2022).
- [33] S. T. Ciocys, N. Maksimovic, J. G. Analytis, and A. Lanzara, Driving ultrafast spin and energy modulation in quantum well states via photo-induced electric fields, *npj Quantum Materials* **7**, 10.1038/s41535-022-00490-2 (2022).
- [34] M. Michiardi, F. Boschini, H.-H. Kung, M. X. Na, S. K. Y. Dufresne, A. Currie, G. Levy, S. Zhdanovich, A. K. Mills, D. J. Jones, J. L. Mi, B. B. Iversen, P. Hofmann, and A. Damascelli, Optical manipulation of rashba-split 2-dimensional electron gas, *Nature Communications* **13**, 10.1038/s41467-022-30742-5 (2022).
- [35] J. Qu, E. F. Cuddy, X. Han, J. Liu, H. Li, Y.-J. Zeng, B. Moritz, T. P. Devereaux, P. S. Kirchmann, Z.-X. Shen, and J. A. Sobota, Screening of polar electron-phonon interactions near the surface of the rashba semiconductor BiTeCl, *Phys. Rev. Lett.* **133**, 106401 (2024).